Direct Determination of the Magnetic Quadrupole Contribution to the Lyman-α_1 Transition in a Hydrogenlike Ion

G. Weber,[1,2,3] H. Bräuning,[1] A. Surzhykov,[1,2] C. Brandau,[1,4] S. Fritzsche,[1,5,6] S. Geyer,[7] S. Hagmann,[1,8] S. Hess,[1] C. Kozhuharov,[1] R. Märtin,[1,2] N. Petridis,[8] R. Reuschl,[1,5,9] U. Spillmann,[1] S. Trotsenko,[1,3] D. F. A. Winters,[1,2] and Th. Stöhlker[1,2,3]

[1]*GSI Helmholtzzentrum für Schwerionenforschung GmbH, 64291 Darmstadt, Germany*
[2]*Physikalisches Institut, Universität Heidelberg, 69120 Heidelberg, Germany*
[3]*Helmholtz-Institut Jena, 07743 Jena, Germany*
[4]*Institut für Atom- und Molekülphysik, Justus-Liebig-Universität, 35392 Giessen, Germany*
[5]*FIAS Frankfurt Institute for Advanced Studies, 60438 Frankfurt am Main, Germany*
[6]*Department of Physics, University of Oulu, 90014 Oulu, Finland*
[7]*Institut für Angewandte Physik, Universität Frankfurt, 60438 Frankfurt am Main, Germany*
[8]*Institut für Kernphysik, Universität Frankfurt, 60438 Frankfurt am Main, Germany*
[9]*ExtreMe Matter Institute EMMI, 64291 Darmstadt, Germany*

(Received 21 July 2010; published 9 December 2010)

We report the observation of an interference between the electric dipole ($E1$) and the magnetic quadrupole ($M2$) amplitudes for the linear polarization of the Ly-α_1 ($2p_{3/2} \rightarrow 1s_{1/2}$) radiation of hydrogenlike uranium. This multipole mixing arises from the coupling of the ion to different multipole components of the radiation field. Our observation indicates a significant depolarization of the Ly-α_1 radiation due to the $E1$-$M2$ amplitude mixing. It proves that a combined measurement of the linear polarization and of the angular distribution enables a very precise determination of the ratio of the $E1$ and the $M2$ transition amplitudes and the corresponding transition rates without any assumptions concerning the population mechanism for the $2p_{3/2}$ state.

DOI: 10.1103/PhysRevLett.105.243002 PACS numbers: 32.30.Rj, 32.50.+d, 32.70.Fw

Hydrogen-like ions are the simplest and most fundamental atomic systems whose study along the isoelectronic sequence provides detailed information about the effects of relativity and quantum electrodynamics on the atomic structure [1–3]. Since these effects are largest for the $1s$ ground state, experimental studies of $L \rightarrow K$ transitions are of paramount importance for such investigations. This is, in particular, true for the domain of high-Z ions where precision measurements of the Lyman-α_1 transition energies are a powerful technique to test the theory of strong field QED [3,4]. Surprisingly, such spectroscopy experiments performed for high-Z ions at relativistic energies revealed a very strong intensity variation as a function of the observation angle and, hence, a large alignment of the $2p_{3/2}$ state. Indeed, a nonstatistical population of the magnetic substates with different projections m_j of the total angular momentum may result in an anisotropic angular distribution and polarization of the emitted x rays [4–6].

This finding motivated detailed experimental and theoretical studies on the population mechanisms and decay dynamics for the excited states of high-Z ions [7]. Recently, it has been found that the properties of the Ly-α_1 radiation can also be influenced by the electronic structure of the ions owing to their coupling to other than just the electric dipole ($E1$) part of the radiation field. For H-like uranium, for example, it has been shown that the interference between the dominant $E1$ and the magnetic quadrupole ($M2$) amplitudes modifies the angular distribution of the Ly-α_1 radiation significantly [8]. While the admixture of the $M2$ amplitude increases the anisotropy parameter by 28%, compared to a pure $E1$ decay, it contributes overall with less than 1% to the total transition rate. This direct observation of the multipole mixing in atomic physics, a well-known effect from nuclear physics that was established several decades ago [9], has resolved a long-standing disagreement between experiment and theory for the case of high-Z ions [10]. Moreover, since the multipole mixing is caused by an interference of the transition amplitudes, it scales quadratically with the nuclear charge Z and therefore still affects mid-Z ions [8]. Apart from the angular distribution of the emitted Ly-α_1 photons, also the linear polarization is expected to be influenced by the admixture of multipoles higher than $E1$. Because of the lack of appropriate instrumentation, however, no polarization measurements for Ly-α transitions have been performed so far for the high-Z domain. This is in contrast to the low- and mid-Z regime for which the linear polarization of the characteristic x-ray transitions has recently been observed by means of crystal spectroscopy [6,11].

In this Letter, we report the first experimental study of the linear polarization of Ly-α_1 radiation following radiative electron capture (REC) into initially bare uranium ions. Two prototype Compton polarimeters designed for the hard-x-ray regime were used in order to investigate the

effect of the $E1$-$M2$ multipole mixing upon the polarization of the Ly-α_1 radiation for which a significant depolarization was predicted recently [12]. In particular, we demonstrate that the determination of the $E1$ and $M2$ transition amplitudes is feasible by combining linear polarization data with a measurement of the angular distribution of the x-ray radiation emitted from H-like ions. In contrast to a study based only on the observation of the angular distribution, no assumption about the population mechanism for the excited state $2p_{3/2}$ state is required anymore. This finding opens a new route for disentangling the population process of the excited ionic state (i.e., radiative electron capture in the present case) from the subsequent decay (i.e., the atomic structure) of the ions. The model-independent and precise determination of the amplitude ratio will stimulate further quantum-electrodynamical calculations on the transition amplitudes of highly charged ions beyond Dirac's theory.

In experiments with highly charged ions, excited ionic states are typically produced by either the capture of electrons or by impact excitation during collisions with different targets or electrons [13]. Owing to the direction of the ion or electron beams in collision experiments, the excited states are generally aligned for any unpolarized target and total angular momentum $j > 1/2$ due to a nonstatistical population of the magnetic sublevels. This alignment is usually described by a set of parameters $\mathcal{A}_k$ that determine both the angular and polarization properties of the decay photons [14]. For the $2p_{3/2} \rightarrow 1s_{1/2}$ transition, for example, the angular distribution of the radiation in the emitter frame is given by

$$W(\theta) \propto 1 + \beta_{20}^{\mathrm{eff}}(1 - \tfrac{3}{2}\sin^2\theta), \tag{1}$$

where $\beta_{20}^{\mathrm{eff}} = \mathcal{A}_2 f_2(E1, M2)/2$ denotes the "effective" anisotropy parameter. Apart from the coefficient $\mathcal{A}_2$, which describes the alignment of the ion and thus the formation of the (excited) state, this effective parameter includes the so-called structure function $f_2(E1, M2) \approx 1 + 2\sqrt{3}a_{M2}/a_{E1}$ that only depends on the atomic structure of the ion and its coupling to the radiation field. In atomic theory, this coupling is typically expressed in terms of the transition amplitudes due to the electric-dipole field, a_{E1}, and those of all higher multipole components. For the x-ray emission from the $2p_{3/2}$ level of hydrogenlike ions, of course, only the $E1$ and $M2$ field components may occur as two indistinguishable decay paths. The alignment parameter

$$\mathcal{A}_2 = \frac{\sigma(\frac{3}{2}, \pm\frac{3}{2}) - \sigma(\frac{3}{2}, \pm\frac{1}{2})}{\sigma(\frac{3}{2}, \pm\frac{3}{2}) + \sigma(\frac{3}{2}, \pm\frac{1}{2})} \tag{2}$$

in Eq. (1) can be written in terms of the cross sections $\sigma(j_n, \mu_n)$ for populating the magnetic substates μ_n [14], and describes thus the "dynamical" part to the angular distribution of the observed radiation.

The linear polarization of the Ly-α_1 radiation is given by [15]

$$P(\theta) = \frac{-\frac{3}{2}\gamma_{20}^{\mathrm{eff}}\sin^2\theta}{1 + \beta_{20}^{\mathrm{eff}}(1 - \frac{3}{2}\sin^2\theta)}, \tag{3}$$

where we have introduced the effective polarization parameter $\gamma_{20}^{\mathrm{eff}} = \mathcal{A}_2 g_2(E1, M2)/2$ with $g_2(E1, M2) \approx 1 - 2/\sqrt{3}a_{M2}/a_{E1}$, analogous to the angular distribution (1) above. Both, studies of the angular distribution and the linear polarization, can be utilized in order to derive information about the $M2$ amplitude relative to the electric-dipole amplitude while relying on a theoretical estimate for the value of $\mathcal{A}_2$ (or vice versa). However, a combined measurement of both properties of the emitted radiation allows an experimental determination of the amplitude ratio a_{M2}/a_{E1} as well as of the alignment parameter $\mathcal{A}_2$.

The experiment was performed at the internal gas jet target of the experimental storage ring at GSI, Darmstadt. After injection into the ring, U^{92+} ions were decelerated to an energy of 96.6 MeV/u and cooled by the electron cooler [4]. The ions then collided with a gas target of H_2 molecules with a typical areal density of about 10^{13} particles/cm^2 [16]. Under these conditions, excited U^{91+} ions in the $2p_{3/2}$ state were formed via the REC process. The subsequently emitted photons were detected by an array of standard solid state Ge(i) x-ray detectors, located at different observation angles, and by two two-dimensional position-sensitive x-ray detectors. The latter detectors were used as Compton polarimeters, located at 35° and 90° with respect to the ion beam axis. Each of the 2D x-ray detectors consist of a planar Ge(i) or a planar Si (Li) crystal which are segmented into horizontal strips at the front and into vertical strips at the back side. This segmentation results in a pseudopixel structure. For the detector at 90°, moreover, a 7 mm-thick Si(Li) crystal with an active area of 64×64 mm^2, divided into 32 strips on each side, was used, while the 35° detector had a 11 mm-thick Ge(i) crystal with an active area of 56×32 mm^2 and 128 strips at the front side and 48 strips at the back side, respectively. Each strip is read out separately and provides time, position, and energy information for the detected photons as well as multihit capability [17,18]. When the beam had passed the interaction chamber, the down-charged U^{91+} ions were separated from the main beam by a dipole magnet and directed onto a multiwire proportional counter with a detection efficiency close to 100%. The signals provided by the particle detector enabled us to measure the x-ray emission in coincidence with electron capture into the projectile.

Standard x-ray detectors were used to obtain the angular distribution of the Ly-α_1 radiation. In order to reduce the systematic uncertainties, the Ly-α_1 line intensities were normalized to the intensity of the nearby, isotropic Ly-α_2 line (see [10,19]). As a consequence of this procedure, the experimental uncertainties are almost entirely due to counting statistics. Figure 1 displays the measured Ly-α_1 angular distribution. The solid line in Fig. 1 was obtained from a least-squares adjustment of Eq. (1) to the

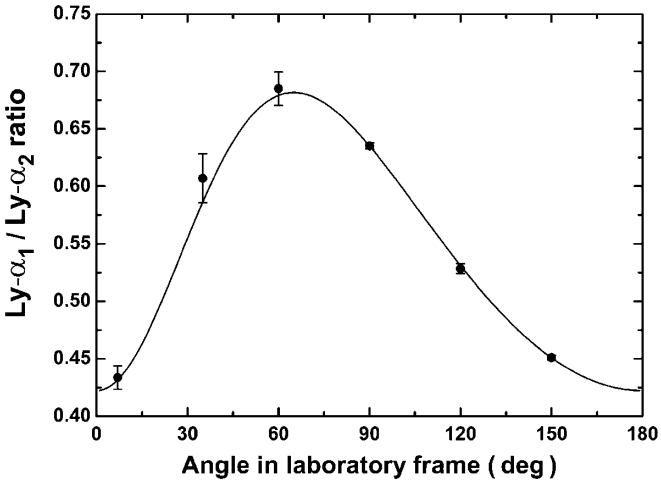

FIG. 1. Normalized angular distribution of the Ly-α_1 radiation following REC into initially bare uranium projectiles with an energy of 96.6 MeV/u. The solid line refers to a least-square adjustment of Eq. (1) to the experimental data, taking the transformation into the laboratory frame into account.

experimental data with the effective anisotropy β_{20}^{eff} taken as free parameter. For this purpose, Eq. (1) was transformed into the laboratory system (see [4,10]). The experimental $\beta_{20}^{\text{eff}} = -0.290 \pm 0.005$, deduced from this fitting procedure, is in good agreement with the value -0.292 from an exact relativistic calculation including the cascade feeding caused by REC into higher levels [8].

By applying the 2D x-ray detectors, the Ly-α_1 linear polarization was obtained by exploiting the polarization sensitivity of the Compton effect described by the Klein-Nishina formula [20] which depends on the incident photon energy E, the polar scattering angle ϑ, and the azimuthal scattering angle φ, respectively, (see also [13,17,18,21–23]). The maximum anisotropy and, thus, polarization sensitivity of the azimuthal scattering distribution occurs at a polar scattering angle of $\vartheta \approx 90°$. Here, the azimuthal scattering cross section is roughly described by a $\cos^2\varphi$ dependence with respect to the incident photon electric field vector. The Klein-Nishina formula can be adjusted to a beam of partially polarized photons by replacing $\cos^2\varphi \rightarrow \frac{1}{2}(1 - P) + P\cos^2\varphi$, where P corresponds to the degree of linear polarization. Thus, the degree of the linear polarization as well as the orientation of the polarization plane of the incident photons can be obtained from the scattered photon angular distribution with respect to the azimuthal angle φ (see [24] for details). In order to obtain this distribution, all events in the 2D x-ray detectors where two inelastic interactions occurred (e.g., Compton scattering followed by photoabsorption of the scattered photon) were analyzed to extract Ly-α_1 Compton events with scattering angles of $\vartheta = 90° \pm 15°$.

Figure 2 shows the 2D distribution of the Compton scattered photons [2D Si(Li) detector] and its projection to the azimuthal angle φ, with each data point corresponding to an arc slice of 11.25°. The error bars are due to

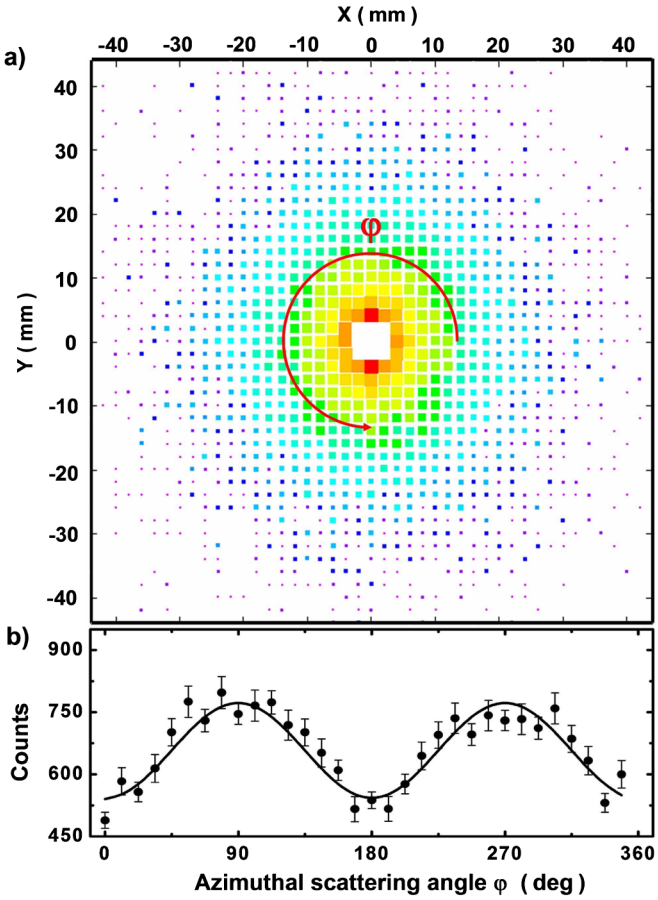

FIG. 2 (color online). (a) Position distribution of the Compton scattered Ly-α_1 photons with respect to the scattering position (0, 0) on the 2D Si(Li) detector. (b) Projection of all scattered photons upon the angle φ in (a). The solid line results from a least-square adjustment of the Klein-Nishina formula modified for partially polarized photon beams to the experimental data (see text).

statistical uncertainties. The incident photon polarization was reconstructed by applying a least-square adjustment of the Klein-Nishina formula modified for partially polarized photons to the data, with the degree of polarization being treated as a free parameter. However, the distribution of the Compton events is altered by several effects such as finite pixel size and limited energy resolution, which all tend to lower the anisotropy with respect to the scattering angle φ. Thus, the polarimeter quality Q of our instruments, defined as the ratio between the degree of linear polarization reconstructed from the detector response and the real incident photons polarization, is less than 1. To correct for these effects, the detector responses were modeled by means of a Monte Carlo simulation based on the EGS5 package, which provides handling of the relevant photon-matter interaction processes [25]. Note, this procedure has already been proven to describe very accurately the detector response of the detectors used and has been discussed in detail in the literature [17]. For both 2D detectors we obtained Q values of at least 0.9, indicating their excellent performance as Compton polarimeters which was demonstrated experimentally in [17].

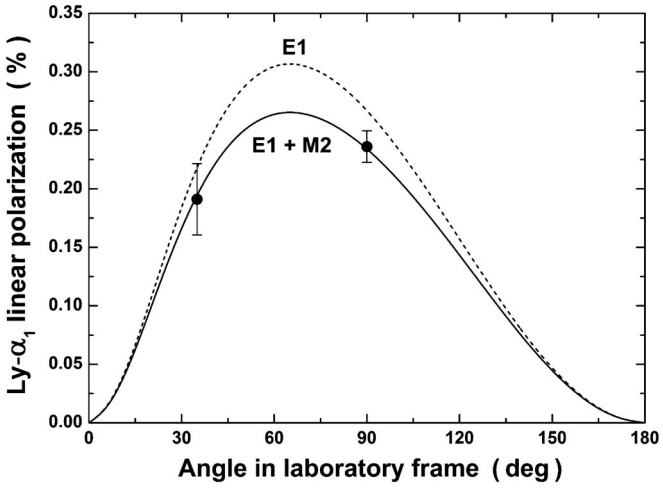

FIG. 3. Measured linear polarization of the Ly-α_1 line following the REC into initially bare uranium projectiles with energy 96.6 MeV/u in comparison to theory with (solid curve) and without (dashed curve) taking into account the $E1$-$M2$ interference.

Figure 3 displays the measured degree of linear polarization of the Ly-α_1 radiation, as observed at 35° and 90° in the laboratory frame, in comparison with theory. The experimental error bars reflect the statistical uncertainty, while the systematic uncertainty is negligible at the present level of statistical accuracy. The two theoretical curves in Fig. 3 were obtained by including only the electric-dipole decay with $f_2(E1, M2) = g_2(E1, M2) = 1$ (dashed line) and within the exact theory that accounts for the corresponding $E1$-$M2$ interference terms (solid line). As seen from this figure, the $E1$-$M2$ multipole mixing reduces the degree of linear polarization by about 15% for observation angles near 90°, compared to the $E1$-only approach, and is in excellent agreement with the experimental data.

As discussed above, combined angular distribution and polarization measurements of the Ly-α_1 radiation removes the need to model the population mechanism of the $2p_{3/2}$ state in order to determine the alignment parameter $\mathcal{A}_2$ and the amplitude ratio a_{M2}/a_{E1}. In Table I, we display these two measured quantities and compare them with theory. As seen from this table, an excellent agreement between experiment and theory is found, where the amplitudes are calculated with relativistic wave functions of a pointlike nucleus, based on Dirac's equation. In particular, we like to point out that our experimental value for the amplitude ratio translates into the ratio for the transition rates of 0.006 89 with an uncertainty of ±2.8%. At this level of accuracy, however, one already expects that the experiment becomes sensitive to the finite nuclear size as well as to QED effects [26]. If, for example, the Dirac value for the transition energy as derived for the pointlike nucleus is replaced by the experimental transition energy (including nuclear size and QED corrections) [3], the computed value for the transition rate ratio changes from 0.007 12 to 0.007 00, i.e., by 1.7%. Taking into account also the influence of these effects to the wave functions may lead to a further alteration of the ratio. This issue will be subject of a detailed theoretical study in the near future.

TABLE I. Comparison of the measured and the theoretical alignment parameter $\mathcal{A}_2$ and $M2$:$E1$ amplitude ratio for the $2p_{3/2}$ level and Ly-α_1 decay of H-like uranium. The theoretical values also include the cascade feeding due to capture into high-lying levels. See text for further discussion.

Alignment parameter $\mathcal{A}_2$		Amplitude ratio a_{M2}:a_{E1}	
Experiment	Theory	Experiment	Theory
−0.451 ± 0.017	−0.457	0.083 ± 0.014	0.0844

The support by the ExtreMe Matter Institute (EMMI) in the framework of the Helmholtz Alliance HA216/EMMI is acknowledged. A. S. acknowledges support from the Helmholtz Gemeinschaft and GSI under the project VH-NG-421 and S. F. acknowledges support from the FiDiPro programme of the Finnish Academy.

[1] T. Udem *et al.*, Phys. Rev. Lett. **79**, 2646 (1997).
[2] G. W. F. Drake, in *The Spectrum of Atomic Hydrogen: Advances* edited by G. W. Series (World Scientific, Singapore, 1988).
[3] A. Gumberidze *et al.*, Phys. Rev. Lett. **94**, 223001 (2005).
[4] J. Eichler and Th. Stöhlker, Phys. Rep. **439**, 1 (2007).
[5] J. H. Scofield, Phys. Rev. A **40**, 3054 (1989).
[6] D. L. Robbins *et al.*, Phys. Rev. A **74**, 022713 (2006).
[7] S. Fritzsche, P. Indelicato and Th. Stöhlker, J. Phys. B **38**, S707 (2005).
[8] A. Surzhykov *et al.*, Phys. Rev. Lett. **88**, 153001 (2002).
[9] K. S. Krane, Phys. Rev. C **10**, 1197 (1974).
[10] Th. Stöhlker *et al.*, Phys. Rev. Lett. **79**, 3270 (1997).
[11] G. K. James *et al.*, Phys. Rev. A **57**, 1787 (1998).
[12] A. Surzhykov *et al.*, Hyperfine Interact. **146–147**, 35 (2003).
[13] Th. Stöhlker *et al.*, Eur. Phys. J. Special Topics **169**, 5 (2009).
[14] E. G. Berezhko and N. M. Kabachnik, J. Phys. B **10**, 2467 (1977).
[15] A. Surzhykov *et al.*, J. Phys. Conf. Ser. **212**, 012032 (2010).
[16] M. Kühnel *et al.*, Nucl. Instrum. Methods Phys. Res., Sect. A **602**, 311 (2009).
[17] U. Spillmann *et al.*, Rev. Sci. Instrum. **79**, 083101 (2008).
[18] G. Weber *et al.*, JINST **5**, C07010 (2010).
[19] Th. Stöhlker *et al.*, Phys. Rev. Lett. **86**, 983 (2001).
[20] O. Klein and Y. Nishina, Z. Phys. **52**, 853 (1929).
[21] S. Tashenov *et al.*, Phys. Rev. Lett. **97**, 223202 (2006).
[22] U. Spillmann, Ph.D. thesis, University of Frankfurt, 2009 (unpublished).
[23] S. Hess, Ph.D. thesis, University of Frankfurt, 2010 (unpublished).
[24] F. Lei, A. J. Dean, and G. L. Hills, Space Sci. Rev. **82**, 309 (1997).
[25] H. Hirayama *et al.*, *The EGS5 Code System*, Stanford, Report No. SLAC-R-730 2005.
[26] M. Hillery and P. J. Mohr, Phys. Rev. A **21**, 24 (1980).